Published in final edited form as:
Skin Res Technol. 2005 August ; 11(3): 179–184. doi:10.1111/j.1600-0846.2005.00117.x.

Detection of asymmetric blotches (asymmetric structureless areas) in dermoscopy images of malignant melanoma using relative color

William V. Stoecker[1,2], **Kapil Gupta**[3], **R. Joe Stanley**[3], **Randy H. Moss**[3], and **Bijaya Shrestha**[2]

[1]The Dermatology Center, Rolla, MO, USA

[2]Division of Dermatology, Department of Internal Medicine, University of Missouri Health Sciences Center, Columbia, MO, USA

[3]Department of Electrical and Computer Engineering University of Missouri-Rolla, Rolla, MO, USA

Abstract

Background—Dermoscopy, also known as dermatoscopy or epiluminescence microscopy (ELM), is a non-invasive, *in vivo* technique, which permits visualization of features of pigmented melanocytic neoplasms that are not discernable by examination with the naked eye. One prominent feature useful for melanoma detection in dermoscopy images is the asymmetric blotch (asymmetric structureless area).

Method—Using both relative and absolute colors, blotches are detected in this research automatically by using thresholds in the red and green color planes. Several blotch indices are computed, including the scaled distance between the largest blotch centroid and the lesion centroid, ratio of total blotch areas to lesion area, ratio of largest blotch area to lesion area, total number of blotches, size of largest blotch, and irregularity of largest blotch.

Results—The effectiveness of the absolute and relative color blotch features was examined for melanoma/benign lesion discrimination over a dermoscopy image set containing 165 melanomas (151 invasive melanomas and 14 melanomas *in situ*) and 347 benign lesions (124 nevocellular nevi without dysplasia and 223 dysplastic nevi) using a leave-one-out neural network approach. Receiver operating characteristic curve results are shown, highlighting the sensitivity and specificity of melanoma detection. Statistical analysis of the blotch features are also presented.

Conclusion—Neural network and statistical analysis showed that the blotch detection method was somewhat more effective using relative color than using absolute color. The relative-color blotch detection method gave a diagnostic accuracy of about 77%.

Keywords

dermoscopy; asymmetric blotches; structureless areas; image analysis; melanoma; dysplastic nevi

Malignant melanoma will have an estimated incidence of 55,100 and an estimated total of 7910 deaths in the United States in 2004 (1). Epiluminescence microscopy (ELM), also known as skin-surface microscopy, dermatoscopy or dermoscopy, practiced by skilled

Address: Dr. Stoecker, The Dermatology Center, 1702 E. 10th St., Rolla, MO 65401-4600, USA, Fax: 573-364-0129, wvs@umr.edu.

observers, offers higher diagnostic accuracy than observation without magnification (2–5). Digital dermoscopy, providing numerical indices from various features using image analysis, allows automatic detection of certain features and diagnostic accuracy that is within the range of the best diagnostic accuracy obtainable by skilled human observers using dermoscopy (6).

A key feature for discrimination of melanoma from nevi is the presence of blotches, also called structureless areas (5, 7, 8). These dark blotchy areas within melanocytic lesions were defined in a virtual dermoscopy consensus meeting as ‘black, brown, and/or gray structureless areas with symmetrical or asymmetric distribution within the lesion’ (5). Figure 1 presents an example of a blotch in a dysplastic nevus dermoscopy image. It has a location that is somewhat eccentric and a shape that is somewhat irregular. Figure 2 shows an example of a blotch in a malignant melanoma dermoscopy image. This blotch is more eccentric in location and is also more irregular in shape. It is the purpose of this paper to describe automatic detection and scoring of asymmetric and irregular blotchy areas.

In this paper, two approaches are used to detect the blotchy areas. The first method uses thresholds placed upon the values of the red, green, and blue (RGB) components of the pixels within the lesions. The second method uses relative color thresholds, subtracting the observed pixel value within the lesion from the background skin color before applying relative thresholds, with the goal of minimizing differences because of cameras, lighting, and other photographic and digitizing techniques (9).

Methods

Pigmented lesions

For blotch algorithm evaluation, 512 dermoscopy images of skin lesions with biopsy confirmation of diagnoses were obtained from two sources. The EDRA Interactive Atlas of Dermoscopy (10) was the source of 97 melanomas, including 14 melanomas *in situ* and 83 invasive melanomas, and 113 dysplastic (Clark) nevi in jpeg format. Skin and Cancer Associates, Plantation, Florida provided images of 124 nevocellular nevi, 105 dysplastic nevi, and 68 invasive malignant melanomas digitized in tiff format. Dermatology Associates of Tallahassee Florida, was the source of five dysplastic nevi digitized in tiff format. The total number of melanomas was 165 and benign nevi 347, with 124 of these nevocellular nevi without dysplasia and 223 of these dysplastic nevi. All jpeg images were converted to tiff format. Manual lesion borders were obtained under the supervision of Dr Stoecker. The difficulty of the set was felt to be moderate. Diagnoses were confirmed by histopathology.

Absolute color blotches

Blotch detection was accomplished by setting absolute thresholds in red and green. Normal skin has a greater red component than blue and green, and so does malignant melanoma. A graph of RGB in the Newton-Maxwell triangle of dysplastic nevi vs. melanoma shows a shift toward the red, on the average, in melanoma (9). The rule $R<120$ and $G<60$ was used for absolute color.

Relative color blotches

The background skin color was found by averaging skin color over the perimeter of the lesion. An area of 10% of the lesion size around the lesion was omitted, to reduce the effect of periborder inflammation and errors in border determination. Areas of nonskin, typically black or white borders, rulers on the images, or reflections from bubbles, were omitted from this sampling, by using six criteria for normal skin: $R>90$, $R>B$, $R>G$, $R<250$, $G<250$, and $B<250$, where R, G and B denote the red, green and blue values, respectively, of the pixel

under consideration. Blotch detection was accomplished by the empirically optimized thresholds: ($R_{skin} - R$>140) OR (($R_{skin} - R$>110) AND ($G_{skin} - G$>140)). The first part of the rule before the 'OR' was used to find the darkest blotches with less erythema, which were detected with the single rule in absolute color. R_{skin} and G_{skin}, respectively, are the red and green averages for the background skin. *R*, *G*, and *B* denote the RGB value of the pixel under consideration.

Globule elimination

Globules can be distinguished from blotches by their smaller size, although two dermoscopy atlases and one consensus conference gave no indication of the maximum size of globules or the minimum size for blotches (5, 7, 8). We estimated that for our images of typically 1024 × 768 resolution, blotches had a size exceeding 800 pixels, on the order of 0.2 mm diameter, so the blotch requirement A_{blotch} >800 was included to eliminate globules.

Blotch features

Six indices were examined to characterize the automatically-detected blotches, as shown in Figs 1 and 2 for a benign and malignant lesion, respectively. These were chosen to measure the degree to which blotches are eccentric in location (index 1), large (indices 2–5) and irregular in shape (index 6), and were chosen to be scale-invariant. The first index was the blotch eccentricity index and is given by

$$E = \frac{D}{\sqrt{A}}, \tag{1}$$

where *D* is the Euclidean distance between the centroid of the largest blotch and the centroid of the lesion and *A* is the lesion area. The second index was the relative size of all blotch areas, obtained by dividing the sum of all blotch areas found by the area of the lesion and is represented as

$$R = \frac{\sum_{i=1}^{n} B_i}{A}, \tag{2}$$

where *n* is the number of blotches for the skin lesion and B_i is the area of blotch *i* within the lesion. The third index was the relative size index for the largest blotch and is denoted as

$$S = \frac{B_{max}}{A}, \tag{3}$$

where B_{max} is the area of the largest blotch region within the skin lesion. The fourth and fifth indices were the size of the largest blotch found (B_{max}) and the number of blotches detected within the lesion (*n*), respectively. The sixth index was the irregularity of the largest blotch and is given by

$$I = \frac{P_{max}}{\sqrt{B_{max}}}, \tag{4}$$

where P_{max} is the perimeter of the largest blotch within the lesion.

Blotch feature evaluation

The blotch features were applied to melanoma/benign lesion discrimination using a leave-one-out standard backpropagation neural network approach. All six features (*E*, *R*, *S*, *n*, B_{max}, *I*) were used as inputs to the neural network. A standard backpropagation neural network with architecture of 6 × 4 × 2 × 1 (6 inputs, 4 nodes in first hidden layer, 2 nodes in second hidden layer, 1 output) was used with neural network training up to 10 epochs (convergence based on RMSE error<0.15). Sigmoid transfer functions at the input and hidden layers and a linear transfer function at the output were implemented. A leave-one-out approach was used for training and testing, where each image of the data set was left out of the training set, the neural network was trained with the remaining images, and the neural network output was computed with the image left out used as the source of input features. The neural network output results were evaluated using a receiver operating characteristic (ROC) curve. The ROC curves were generated by incrementing the neural network output threshold over the neural network output range obtained from the data set and computing the true positive and false negative rates at each threshold.

Experimental results

The means and standard deviations of the six indices obtained for the absolute color and relative color blotch features are shown in Table 1 for the melanomas and benign lesions from the data set examined. The statistical analysis for the blotch indices, including *P*-values and correlation factors, was calculated by SAS (SAS Corporation, Cary, NC, USA) for the six indices, also shown in Tables 1–4. The receiver operating characteristic (ROC) curves for diagnosis of melanoma using the blotch features for absolute and relative colors is shown in Fig. 3. The vertical axis shows the sensitivity for melanoma detection, and the horizontal axis presents the corresponding false alarm rate: 1-specificity.

Discussion

Blotches are not defined precisely in terms of size and color. Accordingly, recognition of blotches suffers in comparison with other features. For nine pattern analysis features, (global pattern, pigment network, dots/globules, streaks, blue-whitish veil, hypopigmentation, regression structures, vascular structures, and blotches), blotch recognition ranked lowest on interobserver agreement in a virtual consensus meeting, with a κ of 0.21 (range 0.21–0.44) (5). This was tied for the lowest interobserver agreement of 23 diagnostic features ranked in the same study, with only the positive features in the Menzies method ranked at this lowest level of interobserver agreement. The presence of irregular blotches, however, ranked fifth of 24 diagnostic features in discriminatory power as measured by odds ratio in the same virtual consensus meeting (5). Of 24 features tabulated, the features with the six highest odds ratios for the diagnosis of melanoma were atypical pigment network (9.0), irregular streaks (5.8), regression structures (5.4), irregular dots/globules (4.8), multicomponent global pattern (4.3), and irregular blotches (4.1). Irregular blotches then, although not precisely defined, and although subject to considerable interobserver differences in identification, appear to be one of the most useful features for melanoma diagnosis in dermoscopy images.

The results of the present study confirm that blotches, particularly eccentric blotches, are useful in discriminating melanoma from benign simulators and that automatic blotch detection is feasible. The ROC curve results in Figure 3 show that the relative color-based blotch indices perform somewhat better than absolute color-based blotch indices for most sensitivity ranges. Better performance at the higher sensitivities (>0.8) implies better

discrimination of melanomas that are more difficult to diagnose by blotches. The ROC curve results highlight the utility of relative color for blotch determination in dermoscopy skin lesion images acquired from different sources.

We may interpret the *P*-value for a variable as a measure of how much evidence we have against the null hypothesis (the hypothesis that there is no difference between our two data sets for that variable). Thus a significant feature has a low *P*-value when the feature values are compared for the class of melanomas vs. the class of benign lesions. In this study, we found that eccentricity of the largest blotch has the lowest *P*-value of the indices studied.

This study lacks automatic border determination (segmentation). Border determination can be done using automated methods, including gradient vector flow snakes (11) and color plane union methods (12). The accuracy varies depending upon the metric used, and is generally within the range of interobserver variation. This study also suffers from the subjective comparison of the blotchy areas found by the absolute and relative color measurements. Thresholds were iteratively adjusted until the blotchy areas found by both methods were felt to be fairly similar. In the majority of the cases, the relative color system found a greater blotch area.

Pellacani et al. (13) also implemented methods to find the absolute and relative dark areas. The authors determine relative dark areas as the darkest area after iterative division of the gray level histogram, using lesion pixels only, at the median value, until four zones are obtained, selecting the gray level zone with the largest luminance range (largest number of gray values) after the two divisions. The darkest zone is the relative dark area. Absolute dark areas are obtained by setting a threshold of 0.130 of the brightness of the surrounding skin and relaxing the threshold iteratively. The authors defined their absolute dark areas by comparing with the surrounding skin value, as we have done for our relative measure. As we have found in the present study, they found that measuring color relative to the surrounding skin produces a better melanoma diagnostic accuracy (74.6%) than computing dark areas using lesion color values alone (71.2%).

In summary, for dermoscopy images of melanomas and benign lesions, using manual borders, we obtained a diagnostic accuracy of about 77%, although the use of different data sets and techniques does not allow direct comparison with other studies. Our findings indicate that the eccentricity of the largest blotch, *E*, may provide more information for melanoma diagnosis than the other measures studied. In addition, determination of blotches by determining color thresholds relative to the surrounding skin appears to provide better diagnostic accuracy in detection of melanoma.

Acknowledgments

This work was supported in part by NIH SBIR grant 1R43 CA-101639-01. The authors wish to thank Harold S. Rabinovitz, M.D., and Armand Cognetta, M.D., for supplying dermoscopy images. Jason Hagerty served as system administrator.

References

1. Jemal A, Tiwari RC, Murray T, et al. Cancer statistics 2004. CA Cancer J Clin. 2004; 54:8–29. [PubMed: 14974761]
2. Nachbar F, Stolz W, Merkle T, et al. The ABCD rule of dermatoscopy. High prospective value in the diagnosis of doubtful melanocytic skin lesions. J Am Acad Dermatol. 1994; 30:551–559. [PubMed: 8157780]

3. Binder M, Schwarz M, Winkler A, et al. Epiluminescence microscopy: a useful tool for the diagnosis of pigmented skin lesions for formally trained dermatologists. Arch Dermatol. 1995; 13:286–291. [PubMed: 7887657]
4. Argenziano G, Fabbrocini G, Carli P, De Giorgi V, Sammarco E, Delfino M. Epiluminescence microscopy for the diagnosis of doubtful melanocytic skin lesions: comparison of the ABCD rule of dermatoscopy and a new 7-point checklist based on pattern analysis. Arch Dermatol. 1998; 134:1563–1570. [PubMed: 9875194]
5. Argenziano G, Soyer HP, Chimenti S, Talamini R, Corona R, Sera F, et al. Dermoscopy of pigmented skin lesions: results of a consensus meeting via the Internet. J Am Acad Dermatol. 2003; 48:679–693. [PubMed: 12734496]
6. Rubegni P, Burroni M, Cevenini G, Perotti R, Dell'Eva G, Barbini P, et al. Digital dermoscopy analysis and artificial neural network for the differentiation of clinically atypical pigmented skin lesions: a retrospective study. J Invest Dermatol. 2002; 119:471–474. [PubMed: 12190872]
7. Stolz, W.; Braun-Falco, O.; Bilek, P.; Landthaler, M.; Cognetta, A. Color atlas of dermatoscopy. London: Blackwell Science Ltd; 1994.
8. Menzies, SW.; Crotty, KA.; Ingvar, C.; McCarthy, WH. An atlas of surface microscopy of pigmented skin lesions: dermoscopy. 2. Sydney: McGraw-Hill Companies, Inc; 1996.
9. Stoecker, WV.; Moss, R.; Perednia, DA.; Umbaugh, SE.; Ercal, F. Visible-light digital imaging in dermatology. In: Stoecker, WV., editor. Computer applications in dermatology. New York: Igaku-Shoin; 1993. p. 100-102.
10. Argenziano, G.; Soyer, HP.; De Giorgi, V., et al. Interactive atlas of dermoscopy. Milan, Italy: EDRA Medical Publishing; 2000.
11. Erkol B, Moss RH, Stanley RJ, Stoecker WV, Hvatum E. Automatic lesion boundary detection in dermoscopy images using gradient vector flow snakes. Skin Research and Technology. 2004; 11:17–26. [PubMed: 15691255]
12. Pagadala, P. MS Thesis. Department of Electrical Engineering, University of Missouri-Rolla; Tumor border detection in epiluminescence microscopy images.
13. Pellacani G, Grana C, Cucchiara R, Seidenari S. Automated extraction and description of dark areas in surface microscopy melanocytic lesion images. Dermatology. 2004; 208:21–26. [PubMed: 14730232]

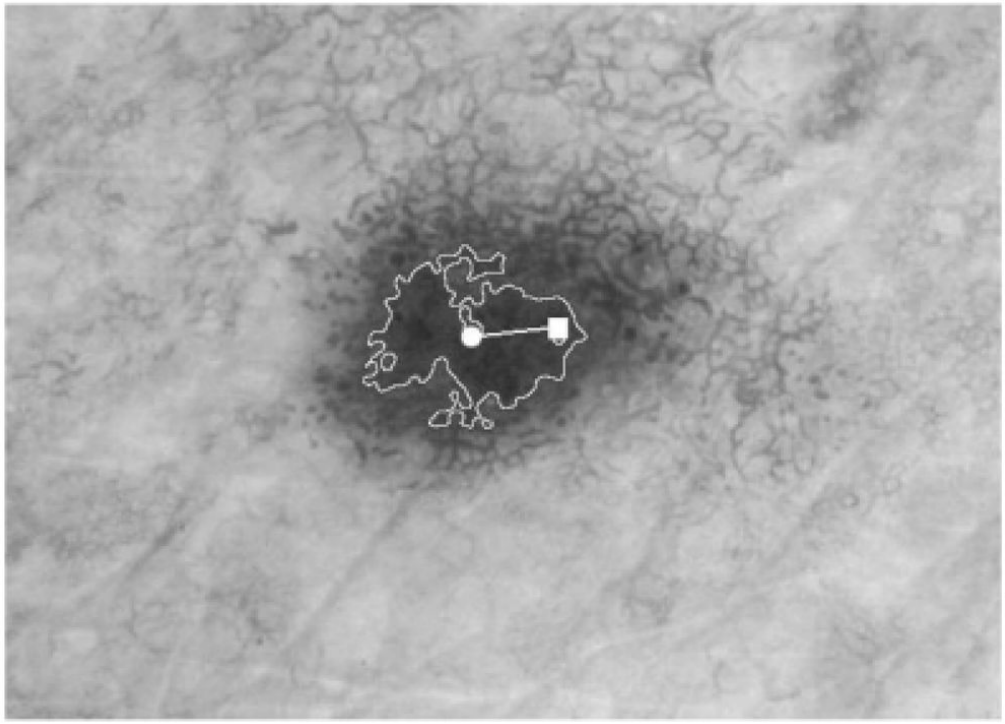

Fig. 1.
Dysplastic nevus with the outline of the largest blotch found automatically, absolute color. The centroid of the tumor is marked with a square; the centroid of the largest blotch is marked with a circle; the intercentroid distance is marked as the line between the two centroids. The eccentricity index is 0.21. The irregularity index is 12.4.

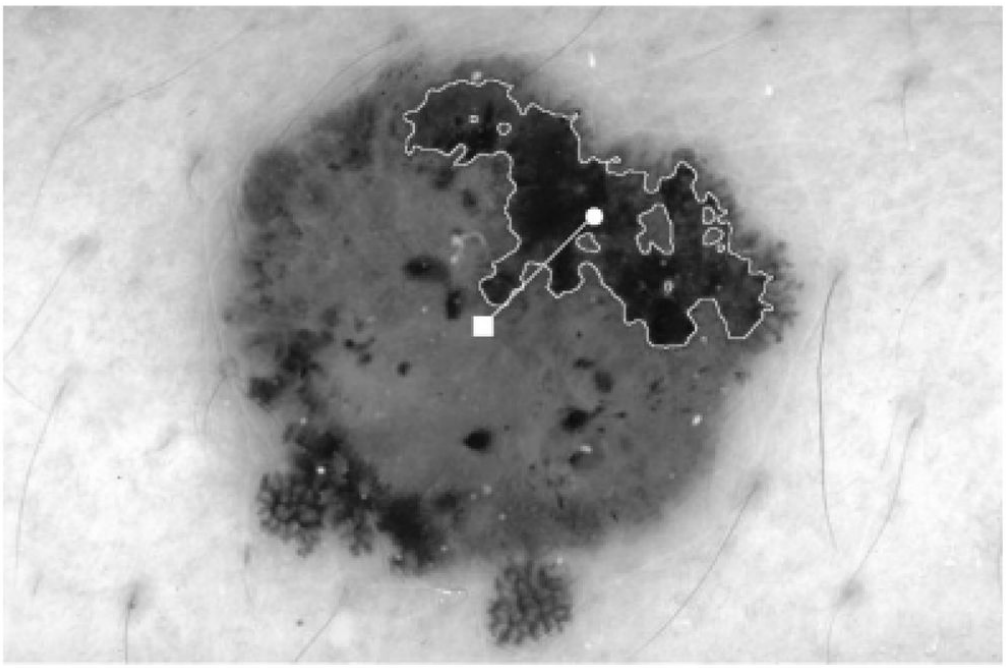

Fig. 2.

Invasive melanoma with the outline of the largest blotch found automatically, absolute color. The centroid of the tumor is marked with a square; the centroid of the largest blotch is marked with a circle; the intercentroid distance is marked as the line between the two centroids. Boundaries for this blotch are sharp and more clearer than for the blotch in Fig. 1. The eccentricity index is 0.30. The irregularity index is 12.8.

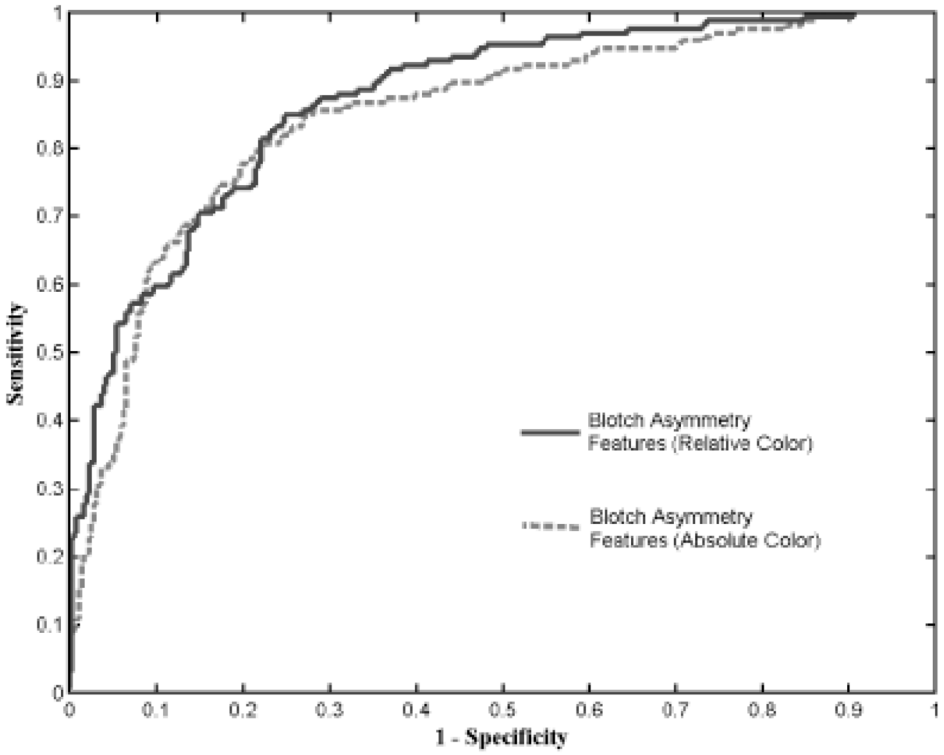

Fig. 3.
Receiver operating characteristic curve for blotch detection with absolute and relative indices. A diagnostic accuracy of about 77% is obtained.

TABLE 1

Absolute indices

Indices	Melanoma	Nevi	*P*-value
E = eccentricity largest blotch	0.174 ± 0.158	0.073 ± 0.12	<0.0001
R = relative area, all blotches	0.180 ± 0.21	0.08 ± 0.15	0.06
S = relative area largest blotch	0.162 ± 0.21	0.07 ± 0.15	0.12
B_{max} = no. of pixels largest blotch	53407.08 ± 123511.64	13350.11 ± 45142.08	0.09
n = no. of blotches	22.07 ± 34.09	9.88 ± 29.84	0.40
I = irregularity largest blotch	10.17 ± 7.11	5.01 ± 7.36	0.88

TABLE 2

Relative indices

Indices	Melanoma	Nevi	*P*-value
E = eccentricity largest blotch	0.177 ± 0.154	0.111 ± 0.135	<0.0001
R = relative area, all blotches	0.29 ± 0.23	0.15 ± 0.20	0.0047
S = relative area largest botch	0.26 ± 0.24	0.14 ± 0.20	0.0765
B_{max} = no. of pixels largest blotch	65435.17 ± 98892.07	29064.67 ± 71848.39	0.7207
n = number of blotches	43.46 ± 81.45	19.30 ± 42.26	0.0894
I = irregularity largest blotch	10.75 ± 6.42	7.72 ± 7.50	0.2782

TABLE 3

Pearson correlations, absolute indices

Indices	***E***	***R***	***S***	B_{max}	***n***	***I***
E = eccentricity largest blotch	1.000	0.030	− 0.027	0.044	0.415	0.544
R = relative area, all blotches	0.030	1.000	0.992	0.607	0.124	0.493
S = relative area largest botch	− 0.027	0.992	1.000	0.598	0.050	0.429
B_{max} = no. of pixels largest blotch	0.044	0.607	0.598	1.000	0.232	0.400
n = number of blotches	0.415	0.124	0.050	0.232	1.000	0.629
I = irregularity largest blotch	0.544	0.493	0.429	0.400	0.629	1.000

TABLE 4

Pearson correlations, relative indices

Indices	*E*	*R*	*S*	B_{max}	*n*	*I*
E = eccentricity largest blotch	1.000	− 0.203	− 0.253	− 0.057	0.409	0.392
R = relative area, all blotches	−0.203	1.000	0.990	0.543	−0.026	0.289
S = relative area largest blotch	−0.253	0.990	1.000	0.530	−0.073	0.240
B_{max} = no. of pixels largest blotch	−0.057	0.543	0.530	1.000	0.272	0.400
n = no. of blotches	0.409	− 0.026	− 0.073	0.272	1.000	0.502
I = irregularity largest blotch	0.392	0.289	0.240	0.400	0.502	1.000